e-ISSN: 2689-4934

Available online at
http://uppp.uitm.edu.my/online-issues.html

ESTEEM Academic Journal Vol 22, March 2026, 17-31

ESTEEM
Academic Journal
(EAJ)

Enhanced purification of supercritical fluid extracts of palm kernel cake phenolics using modified graphene-based adsorbents

Siti Hawa Mat Yaman[1], Norhusna Mohamad Nor[2*], Mohd Azahar Mohd Ariff[3], Ellisa Natasya Rosli[4]

[1, 2, 3, 4]*Chemical Engineering Studies, Universiti Teknologi MARA, Cawangan Pulau Pinang, 13500, Permatang Pauh, Pulau Pinang, Malaysia*

ARTICLE INFO

Article history:
Received 1 December 2025
Revised 16 February 2026
Accepted 10 March 2026
Online first
Published 1April 2026

Keywords:
Adsorption
Graphene Oxide
Hydrophobic Properties
Palm Kernel Cake (PKC)
Purification
Supercritical Fluid Extraction (SFE)

DOI:
10.24191/esteem.v22iMarch.4737

ABSTRACT

This study evaluated the effectiveness of graphene-based adsorbents in purifying phenolic compounds extracted from palm kernel cake (PKC) by supercritical fluid extraction (SFE) at 80 °C, 300 bar, and 42 minutes. Four adsorbents—graphite, graphene oxide (GO), nitrogen-reduced GO (N-rGO), and three-dimensional nitrogen-doped reduced graphene oxide (3D-N-rGO)—were tested under fixed adsorption conditions (30 °C, 1 g adsorbent, 60 min, 300 rpm). Among these, 3D-N-rGO exhibited the highest adsorption capacity (15.47 mg/g), nearly double that of graphite (7.76 mg/g), and achieved the highest desorption ratio (75.58%). It also reduced the total phenolic content from 0.6162 to 0.1927 mg GAE/g bio-oil, representing a reduction of 68.7% . FTIR analysis confirmed the presence of nitrogen-related functional groups (N–H, C=N at ~1550–1650 cm^{-1}) and a reduction in oxygen-containing groups (C=O at ~1720 cm^{-1}, C–O at ~1050–1250 cm^{-1}), indicating successful nitrogen doping and deoxygenation. These structural features enhanced hydrophobicity and selectivity toward phenolic compounds. The findings suggest that 3D-N-rGO shows promise for applications in phytochemical purification, wastewater treatment, and bio-refinery processes. However, challenges such as adsorbent regeneration, material cost, and scalability must be addressed before industrial implementation.

[2*] Corresponding author. *E-mail address*: norhusna8711@uitm.edu.my
https://doi.org/10.24191/esteem.v22iMarch.4737

1. INTRODUCTION

Palm kernel cake (PKC), a significant by-product of the palm oil industry in Malaysia and Indonesia, is a rich source of phenolic compounds with potent antioxidant properties [1]. These bioactives compounds have attracted interest for applications in functional foods, nutraceuticals, cosmetics, and pharmaceuticals due to their metal-chelating ability and free-radical scavenging potential [2]. PKC also contains other valuable compounds, such as terpenes and sterols, further enhancing its potential as a sustainable source of natural ingredients [2]. Supercritical fluid extraction (SFE) is widely used for recovering phenolics from biomass such as PKC because of its efficiency and environmental friendliness. However, the crude extracts obtained via SFE often contain non-phenolic organic compounds, residual solvents, and other contaminants [3]. These impurities may interfere with the biological activity and stability of phenolic compounds, thus affecting their functional performance. Therefore, an effective purification strategy is essential to improve the quality and value of these extracts, enabling their broader use across health-related industries [4]. The relatively high phenolic content in PKC (5.35 mg/g, as reported by Tsouko et al. [2]) highlights its promise as a feedstock for phytochemical recovery, provided that post-extraction purification challenges can be addressed.

Various carbon-based adsorbents, including activated carbon and graphene oxide (GO), have been extensively studied for the removal of phenolic compounds from aqueous and organic media due to their high surface area and abundance of functional groups [5]. GO, in particular, exhibits a strong affinity for phenolics through hydrogen bonding and π–π interactions enabled by its oxygen-containing functionalities [6]. While reduced GO and other GO-based derivatives have been explored to improve adsorption capacity and selectivity [7], their application in purifying complex post-supercritical fluid extraction (post-SFE) streams remains limited. This is primarily due to challenges such as insufficient selectivity in the presence of co-extracted compounds, poor structural stability under supercritical conditions, and limited reusability. Furthermore, many GO-based materials suffer from high synthesis and regeneration costs, which hinder their scalability and economic viability for industrial applications [8]. Although some efforts have been made to enhance GO's adsorption performance—such as incorporating metals, bentonite, or organic moieties—most studies stop short of evaluating their long-term efficiency, recyclability, or performance under SFE-relevant conditions [9]. These limitations underscore a critical need to develope modified graphene-based adsorbents that are more hydrophobic, structurally stable, and recyclable. Such materials could offer enhanced selectivity and cost-effective phenolic recovery in post-SFE purification processes, thereby filling a significant gap in current environmental and separation technologies.

GO adsorbents are hydrophobic and effectively remove phenolic compounds from aqueous solutions. The inherent hydrophobic nature of GO is due to its two-dimensional structure, which consists of nonpolar C=C bonds and the absence of polar functional groups on its outermost layer [10]. This nature enhances strong hydrophobic interactions, including π-π stacking, which facilitate the removal of phenolic compounds. Surface changes, such as the incorporation of hydrophobic moieties or functional groups with chemical affinities, can significantly improve the purification efficacy of GO [11]. Incorporating alkyl or aromatic groups might enhance the adsorbent's affinity for phenolic compounds, rendering GO a flexible material for environmental applications. These alterations facilitate the selective adsorption of diverse phenolic compounds, illustrating the efficacy of graphene-based adsorbents in wastewater treatment and other purification processes.

The interaction of various graphene-based materials with phenolic compounds is significantly affected by the composition and arrangement of functional groups present on their surfaces. GO, characterised by an abundance of oxygen-containing groups such as –OH, –COOH, and epoxide, enhances hydrogen bonding and π–π interactions with phenolic hydroxyl groups and aromatic rings, thereby promoting effective adsorption. In contrast, graphite predominantly depends on π–π stacking attributed to its

https://doi.org/10.24191/esteem.v22iMarch.4737

conjugated basal planes; however, it is deficient in surface functional groups, resulting in comparatively reduced interaction with polar phenolics. Nitrogen-doped reduced graphene oxide (N-rGO), especially when synthesised using chitosan as a nitrogen source, incorporates amine and pyridinic-N groups that improve electrostatic and hydrogen bonding interactions [12]. Meanwhile, 3D-N-rGO, characterised by its porous architecture and elevated nitrogen content, presents a greater surface area and electronic affinity [13]. This advancement not only augments selectivity for phenolic molecules but also optimises diffusion and adsorption kinetics. The structural and chemical characteristics of functionalised graphene materials position them as highly promising candidates for the efficient purification of phenolic compounds from post-SFE extracts.

This work explored various graphene-based adsorbents for the purification of phenolic compounds extracted from PKC and evaluated their adsorption efficiencies. Modification with chitosan is expected to further purify the phenolic compounds in question, most specifically in creating a three-dimensional structure of the 3D-N-rGO adsorbent. No research on the application of 3D-N-rGO for PKC has been conducted in the past five years, highlighting a significant need for further investigation in this area. Several analytical methodologies were added to support the purification process and assess adsorbent performance, such as the determination of the total phenolic content (TPC), whose results quantify phenolic compounds; the adsorption efficiency could be evaluated as well as giving an idea of the phenolics before and after being treated with the adsorbent-that is, the level achieved for purification. This study was conducted to enhance sustainable methods for purifying phenolic compounds and indirectly improve the quality of phytochemical compounds for further use.

2. METHODS

2.1 Materials and chemicals

Throughout the study, various chemicals and materials were identified and used to extract palm kernel cake (PKC), analyse total phenolic content (TPC), and perform the purification process. The PKC was obtained from a local company in Terengganu, Malaysia. The chemicals employed in this study were ethanol (QRec, AR Grade, 96%), liquid Carbon Dioxide, CO_2 (Alpha Gas, 99.9%), Folin-Ciocalteu reagent (QRec, ≥95%), sodium carbonate, Na_2CO_3 (R&M Chemicals, Anhydrous), gallic acid (Sigma-Aldrich, 97.5-102.5% (titration)), graphite powder (Sigma Aldrich, <20μm, synthetic), potassium permanganate, $KMnO_4$ (Sigma Aldrich, ≥99%), hydrogen peroxide, H_2O_2 (QRec, AR Grade, 30-32%), hydrochloric acid, HCl (QRec, AR Grade, 37%), chitosan (Sigma Aldrich, ≥75% deacetylated), and sodium nitrate, $NaNO_3$ (EMSURE).

2.2 Supercritical fluid extraction (SFE) of PKC

PKC extractions were conducted using Supercritical Fluid Extraction (SFE) equipment from Thar Technologies. Inc. by using the method proposed by Ariff et al. [14] with some modifications. The SFE parameters comprised a pressure of 300 bar, a temperature of 80 °C, an extraction duration of 42 minutes, and ethanol as a co-solvent. A total of 15 g of dried PKC was placed in the SFE chamber following the set parameters with a liquid CO_2 flow rate of 25 mL/min. The bio-oil extracts were depressurised and collected in an amber bottle before being stored in a refrigerator at or below 10 °C.

2.3 Adsorbents preparation

Graphene Oxide (GO) was produced using a modified Hummer's method proposed by Javed et al. [15], which involved oxidising the graphite powder. A total of 2.5 g of graphite powder was stirred in 60 mL of

https://doi.org/10.24191/esteem.v22iMarch.4737

concentrated H_2SO_4, and 1.25 g of $NaNO_3$ was gradually added**.** The solution was be rapidly agitated in an ice-water bath at 0–10 ºC for one hour, and to prevent a temperature rise, 7.5 g of $KMnO_4$ was progressively introduced. The solution was vigorously stirred for one hour at less than 20ºC. After stirring at room temperature overnight, the solution turned brown. Then, 135 mL of DI water was slowly added, heated to 60 °C in an oil bath for one hour, and cooled to room temperature. A total of 25mL H_2O_2 was added to stop the reaction, causing the fluid to change from brown to bright yellow. The solution was filtered and washed twice with 400 mL HCl to eliminate the remaining metal ions. The pH was adjusted to 5-6 by washing the solution three times with DI water. The produced GO was dried in an oven at 60 °C for later use. All procedures for the modified Hummer's method were carried out in a fume hood with appropriate personal protective equipment (PPE), including gloves, a lab coat, and goggles, to ensure laboratory safety. All liquid and solid waste was collected in labelled containers and handled following the institution's hazardous waste disposal protocols.

Furthermore, nitrogen-reduced graphene oxide (N-rGO) was synthesised using a one-pot method by Subramaniam et al. [16] with some modifications. Approximately 1 g of GO and 8 wt.% of chitosan were weighed and mixed in 100 mL of distilled water. The mixture was agitated for approximately one hour at 300 rpm at ambient temperature. Subsequently, it was dried in an oven at 80 °C for 24 hours. The dry N-rGO was obtained and then crushed using a mortar. Lastly, 3D-N-rGO was prepared by using microwave-assisted synthesis by Rahim et al with some modifications [17]. In this process, 2 g of glucose were mixed with 2 g of N-rGO in a round-bottom quartz flask. The mixed powder underwent microwave heating at a power setting of 850 W for 30 minutes while nitrogen gas was continuously fed into the quartz flask. The introduction of nitrogen gas during this process resulted in the creation of an inert atmosphere, which helps to avoid the oxidation of the Three-dimensional Nitrogen-reduced Graphene Oxide (3D-N-rGO). The prepared adsorbents were designated as GO, N-rGO, and 3D-N-rGO and were properly stored for use in batch adsorption experiments. Graphite was used as a control to verify the performance improvements of the modified graphene-based adsorbents.

2.4 Batch adsorption and desorption

Purification of phenolic compounds was performed using batch adsorption experiments with some modifications [18]. The experiments were conducted in 100 mL conical flasks sealed with parafilm. The extracted bio-oil solutions containing phenolic compounds were stirred with 1 g of GO adsorbent at 300 rpm for 60 minutes on a heating plate set at 30 °C. The selection of 1.0 g of adsorbent was based on typical dosages reported in previous studies involving graphene-based materials for phenolic compound adsorption. Additionally, 1.0 g provided sufficient adsorbent surface area relative to the extract volume, ensuring complete interaction and avoiding excessive material use. After the adsorption processes was completed, the entire mixtures was filtered to separate the adsorbent from the extracted sample. The filtered extracted sample was referred to as impurities, and ethanol was removed from the palm kernel cake extract using a BUCHI Rotary Evaporator system (Rotavapor R-215, Vacuum Pump V-710, Vacuum Controller V-850, and Chiller F-100).

Subsequently, desorption was performed using 50 mL of acetone as a solvent to release the phenolic compounds adsorbed onto the GO. The desorption process was conducted under the same conditions as the adsorption process. Adsorbents used in the adsorption step, including 3D-N-rGO and others, were stirred in 50 mL of acetone at 300 rpm and 30 °C for 60 minutes. After the desorption process, acetone was removed using the same BUCHI Rotary Evaporator system at a water bath temperature of 50 °C and a rotation speed of 120 rpm. The concentrations of phenolic compounds before and after both adsorption and desorption were determined using Total Phenolic Content (TPC) analysis. The batch adsorption/desorption method was replicated for graphite, N-rGO, and 3D-N-rGO adsorbents. Furthermore, the adsorption

https://doi.org/10.24191/esteem.v22iMarch.4737

capacity, desorption capacity, and desorption ratio were calculated by using Eq. (1), Eq. (2), and Eq. (3), respectively.

$$\text{Adsorption capacity, } Q_e \text{ (mg/g)} = \frac{(C_i - C_f)V_s}{m} \quad (1)$$

$$\text{Desorption capacity, } Q_d \text{(mg/g)} = \frac{C_d V_d}{m} \quad (2)$$

$$\text{Desorption ratio (\%)} = \frac{C_d V_d}{(C_i - C_f)V_s} \times 100\% \quad (3)$$

where C_i (mg/L) represents the initial concentration of the extracted sample, C_f (mg/L) represents the final concentration, C_d (mg/L) represents the sample concentration in the desorption solution, V_s (L) represents the sample solution during the adsorption process, V_d (L) represents the sample solution volume during the desorption process and m (g) represents mass adsorbent used.

2.5 Total phenolic content (TPC)

The Folin–Ciocalteu colorimetric method was applied to assess TPC in the PKC's extracts, with modifications to a previously reported method [19]. Standard gallic acid solutions owere prepared and diluted at the concentrations of 50, 100, 250, and 500 mg/L. Samples were generated in triplicate by mixing 3.16 mL of distilled water, 0.2 mL of Folin-Ciocalteu reagent, 0.6 mL of a 7.5% (w/v) $NaCO_3$ solution, and 0.04 mL of PKC's extracted sample in amber bottles. For the preparation of the blank sample and the calibration curve, ethanol and gallic acid were used, respectively. Themixtures were incubated at ambient temperature for 90 minutes, and then it was assessed at 765 nm with a UV-visible spectrophotometer (DR6000 UV-Vis Spectrophotometer). Eq. (4) was used to calculate the TPC as mg of gallic acid equivalent (GAE) per g of bio-oil extract as follows:

$$\text{Total phenolic content, C (mg GAE/g bio-oil)} = \frac{c \times V}{m} \quad (4)$$

where c is the concentration of gallic acid obtained from the calibration curve in mg/L, V is the volume of extract in L, and m is the mass of extract in grams.

2.6 Fourier transform infrared spectroscopy (FTIR)

The functional groups in the samples were identified using Fourier Transform Infrared Spectroscopy (FTIR) based on their characteristic absorption wavelengths. The analysis was carried out using an FTIR spectrometer (Thermo Scientific, Nicolet iS10 model) over a spectral range of 4000 to 400 cm^{-1} at a resolution of 16 scans. For sample preparation, approximately 1 – 2 mg of dried sample was finely ground and mixed with approximately100 mg of dry potassium bromide (KBr) powder. The resulting mixture was then pelletised using a hydraulic press to form a transparent disc suitable for transmission-mode analysis, following the method outlined by Subramaniam et al. [16].

https://doi.org/10.24191/esteem.v22iMarch.4737

3. RESULTS AND DISCUSSION

3.1 Adsorption – desorption analysis of phenolic compounds

The adsorption and desorption capacities of the tested adsorbents—Graphite, GO, N-rGO, and 3D-N-rGO—exhibited substantial differences, primarily attributed to their distinct structural and surface chemistries (Fig. 1). Among these, 3D-N-rGO emerged as the most effective material, highlighting its potential for efficient adsorption and regeneration processes. These results underscore the importance of both nanoscale architecture and surface modification in optimising adsorbent performance for the recovery of phenolic compounds.

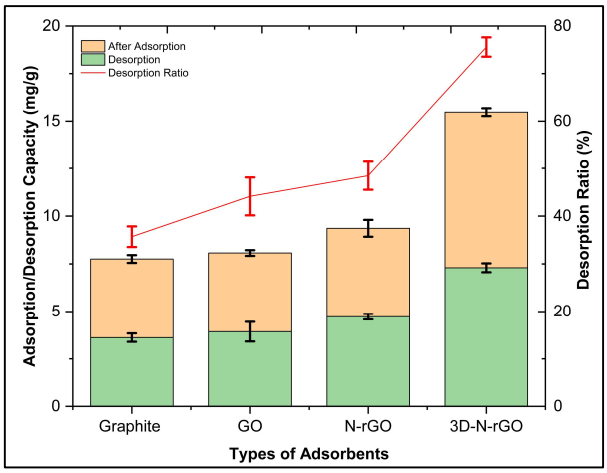

Fig. 1. Adsorption and desorption capacities with desorption ratio for various adsorbents

Graphite, which was used as the control adsorbent, exhibited the lowest performance with an adsorption capacity of 7.76 mg/g, desorption capacity of 3.62 mg/g, and a desorption ratio of 35.69%. These relatively low values reflect the inherent limitations of unmodified graphite, mainly due to its compact and hydrophobic layered structure, as well as its limited surface functional groups, which restrict interactions with polar phenolic compounds. Previous studies have shown that structural modifications,such as exfoliation or functionalization,can enhance its sorption performance. For instance, Movafaghi Ardestani et al. [20] reported an adsorption capacity of 150 mg/g for mercury ions using functionalised expanded graphite, citing increased surface area and oxygenated active sites. Similarly, Tian et al. [21] reported a Congo Red removal efficiency of 87.2% using expanded graphite composites, highlighting the role of porosity and surface modification in improving adsorption performance. While these examples target different pollutants, they reinforce the need for structural enhancement in graphite-based adsorbents.

Graphene oxide (GO) showed moderate improvement over graphite, with an adsorption capacity of 8.07 mg/g and desorption capacity of 3.94 mg/g, along with the highest desorption ratio of 44.14% among the tested materials. This improvement is attributed to the presence of abundant oxygen-containing functional groups, such as hydroxyl, carboxyl, and epoxide, which enhance hydrophilicity and increase the number of accessible active sites. Consistence with this finding, Phatthanakittiphong and Seo [22] reported rapid adsorption–desorption kinetics for bisphenol A using GO (49.26 mg/g), supported by its expandable interlayer spacing and surface functionalisation. Similar findings were observed by Luong et al., who

https://doi.org/10.24191/esteem.v22iMarch.4737

developed a graphene oxide–chitosan composite that demonstrated high adsorption efficiency, achieving 97% removal of methylene blue in the first cycle [23].

N-rGO exhibited a notable adsorption capacity of 9.36 mg/g for phenolic compounds, which can be primarily attributed to nitrogen doping, which enhances π–π stacking and hydrogen bonding interactions with phenolic molecules. Despite this high adsorption performance, its desorption capacity was limited to 4.73 mg/g, with a desorption ratio of 48.47%, suggesting the presence of strong adsorbate–adsorbent interactions that may hinder reusability. Compared with GO, N-rGO demonstrated superior performance due to its high mesoporosity (72.9%), hydrophobic surface characteristics, and partially graphitised carbon structure, all of which promote stronger interactions with hydrophobic organic molecules [24]. Song et al. reported that N-rGO achieved adsorption capacities of 5.77 mg/g for anthracene and 9.29 mg/g for 2-methylanthraquinone, representing increases of 2.76- and 2.29-fold, respectively, compared with GO. These findings further confirm the material's enhanced affinity resulting from surface and structural modifications [24]. Nitrogen doping has also been shown to introduce surface defects and increase the density of active sites, thereby further enhancing adsorption efficiency. Although GO contains oxygen-rich functional groups that contribute to its hydrophilic character, potentially limiting its interaction with hydrophobic phenolics, the nitrogen functionalities in N-rGO increase electron density and create donor–acceptor interaction sites more favourable for phenolic binding. Furthermore, Utami et al. found that rGO-based composites, such as N–doped TiO_2 into rGO, have demonstrated improved photocatalytic properties, including visible-light responsiveness and enhanced charge transfer, with removal efficiencies as high as 96%. This reinforces the versatility and effectiveness of rGO-derived materials in environmental remediation [25].

In contrast, 3D-N-rGO, the main focus of this study, demonstrated significantly superior performance, with an adsorption capacity of 15.47 mg/g, which more than double that of graphite. This enhancement is due to its unique three-dimensional porous structure and nitrogen doping, which together increase surface area, improve porosity, and provide a higher density of functional sitesfor phenolic adsorption. These findings are consistent with earlier studies, such as Jain et al. [13], who reported a phenol adsorption capacity of 204.24 mg/g using GO/CNT hybrid aerogels. The superior performance of 3D-N-rGO can be attributed to its ability to create a more accessible surface area through its 3D network, allowing for more interaction with adsorbates. In addition, nitrogen doping introduces functional groups that enhance the material's interaction with phenolic compounds, thereby improving its overall adsorption efficiency. This is similar to the findings of Tee et al., who developed a phosphorus-doped 3D graphene oxide with bentonite and carboxymethyl cellulose crosslinking (PG/BCC), which achieved a remarkable adsorption capacity of 458.95 mg/g for imipramine under optimised conditions. These findings further support the view that structural modifications significantly enhance the adsorption capabilities of 3D materials [26].

3.2 Total phenolic content (TPC) analysis

The total phenolic content (TPC) of bio-oil, both before and after purification using different adsorbents—graphite, GO, N-rGO, and 3D-N-rGO—exhibited varying levels of purification efficiency, as shown in Fig. 2. Before purification, the TPC was consistent across all samples at 0.616 mg GAE/g bio-oil, ensuring a fair comparison among the different adsorbents. After treatment, graphite showed the lowest adsorption performance, reducing the TPC to 0.4821 mg GAE/g bio-oil. This lower efficiency can be attributed to graphite's limited surface area, absence of oxygen-containing functional groups, and poor dispersion in ethanol, which hinders its ability to interact with polar phenolic compounds. In contrast, GO achieved a more significant reduction to 0.3667 mg GAE/g bio-oil. According to Anegbe et al., GO has attracted considerable attention for its potential in adsorption and purification applications due to its large surface area, high adsorption capacity, and chemical stability [27]. These properties are further enhanced by the presence of oxygenated functional groups, such as hydroxyl, epoxy, and carboxyl groups,which

https://doi.org/10.24191/esteem.v22iMarch.4737

promote stronger hydrogen bonding, π–π stacking, and polar interactions with organic compounds such as phenolics in ethanol [28]. In a related study, Baratta et al. examined the performance of graphene oxide/single-walled carbon nanotube (GO-SWCNT) composite membranes in removing organic compounds, specifically non-steroidal anti-inflammatory drugs (NSAIDs), from water. The study found that the adsorption capacity of the GO-SWCNT composite membranes was significantly affected by the graphene oxide content, with the highest capacities observed at 75 wt.% graphene oxide.

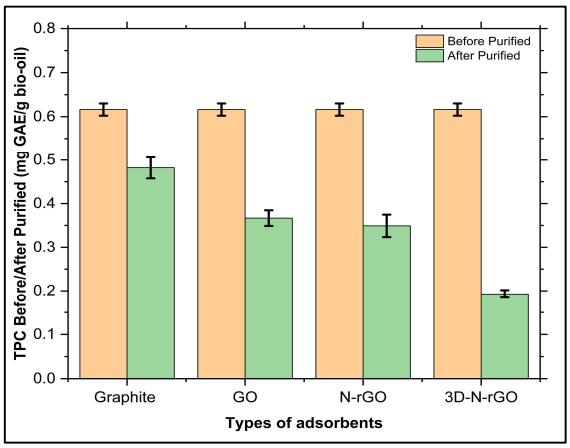

Fig. 2. Total phenolic content (TPC) in bio-oil before and after purification using different adsorbents

N-rGO significantly enhanced the purification process, lowering the TPC from 0.6162 to 0.3490 mg GAE/g bio-oil. Nitrogen doping introduced additional functional groups, such as amine and pyridinic nitrogen, which interact more effectively with phenolic compounds, thereby improving adsorption performance compared to GO. The presence of nitrogen also increases surface polarity and electron-donating capability, enhancing the material's affinity toward polar organic compounds like phenolics. This provides N-rGO with a notable advantage over GO, which primarily depends on oxygenated groups for adsorption. These improvements are in line with the findings of Wu et al. [29], who demonstrated that nitrogen doping in reduced graphene oxide enhanced adsorption capacity and surface polarity, achieving over 90% degradation of sulfamethoxazole via a synergistic adsorption–catalytic oxidation mechanism. Similar trends were observed by Khaliha et al. [30], where reduced graphene oxide (rGO) exhibited greater adsorption of perfluoroalkyl substances (PFASs), achieving 138 µg/g removal compared to 72 µg/g with GO. These findings underscore the superior adsorption performance of nitrogen-doped or reduced graphene-based materials, further validating the effectiveness of N-rGO in capturing phenolic compounds from bio-oil.

In this study, 3D-N-rGO demonstrated enhanced adsorption performance compared to N-rGO for the purification of phenolic compounds from palm kernel cake (PKC) extract. It reduced the total phenolic content (TPC) from 0.6162 to 0.1927 mg GAE/g bio-oil, achieving a 68.7% reduction, compared to N-rGO, which reduced it only to 0.3490 mg GAE/g bio-oil (43.4% reduction). This significant difference is due to the 3D-N-rGO's interconnected porous network, which provides greater surface area and diffusion pathways, thereby improving contact with phenolic molecules and reducing pore blockage. These structural advantages promote more efficient mass transfer and a higher adsorption capacity. Similar benefits of 3D graphene-based materials were reported by Jayakumar et al. [31], who showed that a self-healing 3D-rGO nanoarray significantly enhanced the electrochemical detection of bisphenol A (BPA), due to its high

https://doi.org/10.24191/esteem.v22iMarch.4737

surface area and improved electron/molecule transport. Their findings support the concept that three-dimensional architectures improve interaction efficiency with target compounds.

3.3 Effectiveness of 3D-N-rGO in phenolic compound purification

The effectiveness of 3D-N-rGO in purifying phenolic compounds from palm kernel cake (PKC) extract is clearly illustrated in Fig. 3. The use of nitrogen-doped three-dimensional graphene-based adsorbents enhances adsorption through multiple mechanisms, particularly chemisorption dominated by π–π interactions and hydrogen bonding. Additionally, thermodynamic analysis from previous studies has indicated that such adsorption processes are endothermic and spontaneous, supporting their efficiency and reliability [32]. These findings align with the trends observed in this study, where the hierarchical architecture and chemical modification of 3D-N-rGO significantly outperformed conventional N-rGO. This approach strengthens ongoing efforts to develop high-performance graphene-based adsorbents tailored for bio-oil quality enhancement through the removal of phenolic compounds.

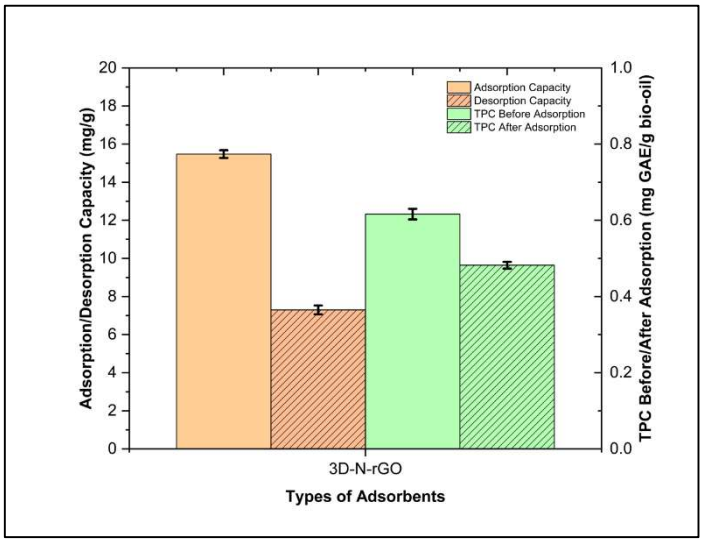

Fig. 3, Summary of performance 3D-N-rGO in adsorption/desorption PKC extract.

The exceptional performance of 3D-N-rGO in purifying bio-oil is demonstrated by its high adsorption capacity of 15.47 mg/g and a significant reduction in total phenolic content (TPC) from 0.6162 to 0.1927 mg GAE/g, corresponding to a 68.7% decrease. Its relatively low desorption value of 7.30 mg/g and high desorption ratio of 75.58% suggest strong retention of phenolic compounds, likely driven by a combination of π–π stacking, hydrogen bonding, and hydrophobic interactions between nitrogen-functionalised graphene layers and the adsorbed molecules. These interactions contribute to the formation of stable adsorption complexes that resist desorption. Superior performance is further attributed to the material's engineered three-dimensional architecture, which enhances mass transfer, increases accessibility to active sites, and facilitates more effective surface interactions. Additionally, nitrogen doping introduces reactive functional groups that improve affinity for organic polar compounds such as phenolics. These findings align with previous work by Gong et al. [33], who demonstrated that 3D nitrogen-doped graphene quantum dot/rGO composites achieved enhanced adsorption due to the synergistic effects of heteroatom doping and structural optimisation.

https://doi.org/10.24191/esteem.v22iMarch.4737

3.4 Surface functional groups of graphene-based adsorbents

FTIR is used to identify the functional groups in phenolic compounds and confirm the structural modifications of adsorbents, thereby ensuring that chemical interactions between the adsorbents and phenolic compounds are well characterised. The FTIR spectrum of graphite, GO, N-rGO and 3D-N-rGO (Fig. 4) explains their respective characteristic peaks at a wavelength from 400 to 4000 cm^{-1}. The FTIR spectrum of graphite presents few peaks, which is consistent with its highly crystalline, sp^2 hybridised carbon structure with low surface functionality. The absence of a strong peak at 3418 cm^{-1} confirms the low presence of O–H stretching and hydroxyl (-OH) groups, indicating that the graphite has not undergone significant oxidation. The aromatic C=C stretching corresponds to a sharp absorption band at 1632 cm^{-1}, which ascertains the presence of intact sp^2 carbon bonds within the graphene layers. Moreover, the absence of peaks around 1700 and 2920 cm^{-1} suggests the absence of carbonyl (-C=O) and aliphatic C–H bonds in the sample, confirming that the samples do not bear any oxygen-containing groups and hydrocarbon contamination. These features agree with the properties expected of pure, unfunctionalised graphite: a prominent conjugated aromatic structure and hardly any IR-active functional groups.

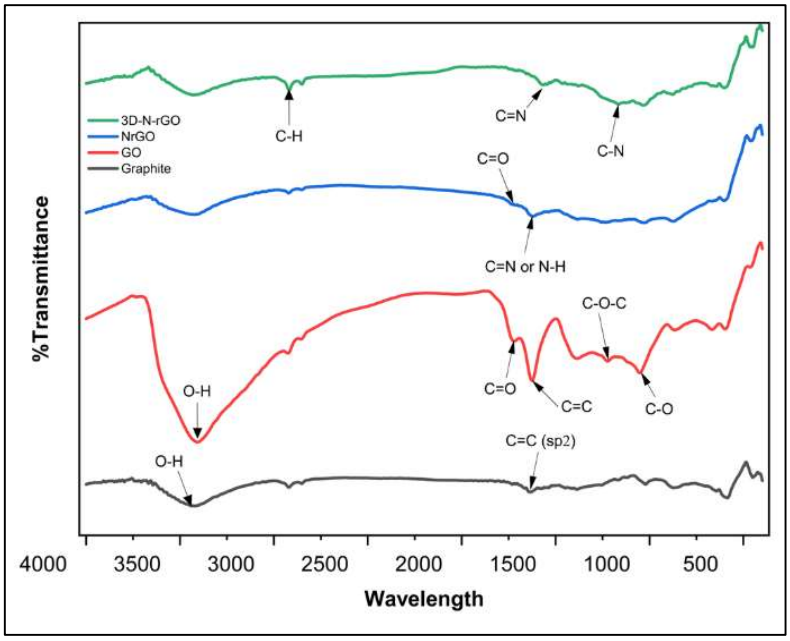

Fig. 4. FTIR analysis for graphene-based adsorbents

By contrast, the FTIR spectrum of GO indicated successful oxidation evidenced by the well-defined peaks for the oxygen-containing functional groups. A broad band near 3400 cm^{-1} corresponds to O–H stretching, indicating hydroxyl groups on the basal planes and edges of the GO sheets. The strong peak at approximately1720 cm^{-1} is attributed to C=O stretching, likely from carboxylic acids or ketones introduced during the oxidation process [34]. The absorption band at 1600 cm^{-1} represents C=C stretching of the remaining sp^2 hybridised carbon, indicating that some aromatic domains remain intact. These peaks in the 1000–1300 cm^{-1} range are attributed to the C–O–C (epoxy) [35] and C–O (alkoxy) [35] bonds, confirming the presence of epoxy and alkoxy groups on the basal plane. These observations are in agreement with those reported by Tang et al. [35], who found that the FTIR spectrum of GO exhibited strong signals

https://doi.org/10.24191/esteem.v22iMarch.4737

corresponding to O–H, C=O, and C–O bonds, indicating the disruption of the sp^2 carbon network and the incorporation of oxygen functionalities into the GO matrix.

FTIR spectra for N-rGO and 3D-N-rGO display apparent differences. The broad peak of N-rGO at around 3421 cm^{-1} can be assigned to the O–H and N–H stretching vibrations, indicating the presence of nitrogenous functional groups that have been introduced by chitosan. The peak near 1620 cm^{-1} is due to the C=C stretching of aromatic domains, and at 1560 cm^{-1}, a peak corresponds to the C=N or N–H bending vibrations, thereby confirming successful nitrogen doping. The reduced intensity of peaks at around 1700 cm^{-1}, assigned to C=O stretching, indicates the reduction of oxygen-containing groups, confirming effective reduction [34]. The FTIR spectrum of 3D-N-rGO shows a stronger signal within the range of 1564 cm^{-1}, corresponding to C=N or amide linkages, which suggests that the three-dimensional structure favours nitrogen doping and retention [35]. This observation is supported by Tang et al. [35], who incorporated polyaniline (PANI) into graphene-based hydrogels and reported distinct FTIR peaks at 1590, 1480, 1307, and 800 cm^{-1}characteristic of PANI—indicating successful integration and nitrogen functionalisation. Their study demonstrated that the hydrogel framework promotes stronger bonding and nitrogen retention, reinforcing the role of 3D structures in enhancing nitrogen doping efficiency. This is further corroborated by Tian et al. [36], who reported C=N stretching at 1575 cm^{-1} in N-doped rGO/waterborne polyurethane composites, highlighting that the presence of C=N bonds is a reliable indicator of successful nitrogen incorporation through chemical interaction with the host matrix.

The synthesis of such materials is ascertained by the presence of nitrogen-functionalised groups and a reduction of oxygen-containing species. The 3D structure of 3D-N-rGO enhances its potential for adsorption and energy storage applications due to its porous, interconnected network that improves surface accessibility and molecular diffusion. These functional groups play a critical role in the purification process because the nitrogen-containing functional groups, C=N and N–H, increase interactions with phenolic compounds, while the reduced oxygen groups increase hydrophobicity, thus assisting in the selective capture of phenolic impurities. This structural design elucidates the considerable decrease in total phenolic content (TPC) from 0.7223 mg GAE/g to 0.3119 mg GAE/g in the bio-oil, showcasing the exceptional purification capability of phenolic compounds by 3D-N-rGO.

4. CONCLUSIONS

This study shows the significant effectiveness of hydrophobic graphene-based adsorbents, specifically 3D nitrogen-doped reduced graphene oxide (3D-N-rGO), in the purification of phenolic compounds derived from palm kernel cake (PKC) using supercritical fluid extraction (SFE). Among the tested adsorbents, 3D-N-rGO demonstrated exceptional performance, achieving the highest adsorption capacity (15.47 mg/g) and a significant decrease in total phenolic content (TPC) from 0.6162 to 0.1927 mg GAE/g bio-oil, signifying its efficacy in eliminating impurities while preserving vital bioactive compounds. The increased efficiency is due to its distinctive three-dimensional structure, nitrogen doping, and greater surface area and porosity, which offer numerous active sites for adsorption. The FTIR analysis confirmed the structure transformation across graphene-based adsorbents. GO had strong peaks for the oxygen-containing groups, O–H stretching at 3400 cm^{-1}, C=O stretching at 1720 cm^{-1}, and C–O stretching between 1000–1300 cm^{-1}, indicating successful oxidation. On the contrary, N-rGO and 3D-N-rGO had reduced intensities of these peaks with the appearance of new peaks for N–H and C=N stretching between 1550–1650 cm^{-1}, thus indicating successful reduction and nitrogen doping, particularly for 3D-N-rGO. The enhanced performance of 3D-N-rGO is believed to be because of its three-dimensional porous structure, nitrogen doping, and increased surface area, offering many active sites for adsorption. This study outlined the promise of 3D-N-rGO as a pivotal material in the domain of sustainable bio-oil purification processes and encouraged further investigation into its scalability and wider industrial applications.

https://doi.org/10.24191/esteem.v22iMarch.4737

5. ACKNOWLEDGEMENTS

This research was supported by the Ministry of Higher Education (MOHE) through the Fundamental Research Grant Scheme (Grant No. FRGS/1/2022/TK0/UITM/02/100). The authors are grateful for the facilities provided by Universiti Teknologi MARA (UiTM) Cawangan Pulau Pinang in the completion of this work.

6. CONFLICT OF INTEREST STATEMENT

The authors agree that this research was conducted in the absence of any self-benefits, commercial or financial conflicts and declare the absence of conflicting interests with the funders.

7. AUTHORS' CONTRIBUTIONS

Siti Hawa Mat Yaman: Conceptualisation, methodology, formal analysis, investigation, and writing-original draft; **Norhusna Mohamad Nor**: Conceptualisation, supervision, writing- review and editing, and validation; **Mohd Azahar Mohd Ariff**: Conceptualisation, methodology, and formal analysis; **Ellisa Natasya Rosli**: Methodology and formal analysis

8. REFERENCES

[1] N. F. Azman *et al.*, "Utilization of palm kernel cake as a renewable feedstock for fermentative hydrogen production," *Renew. Energy*, vol. 93, pp. 700–708, Aug. 2016. Available: https:// doi.org/ 10.1016/j.renene.2016.03.046

[2] E. Tsouko, M. Alexandri, K. Vieira Fernandes, D. Maria Guimarães Freire, A. Mallouchos, and A. A. Koutinas, "Extraction of Phenolic Compounds from Palm Oil Processing Residues and Their Application as Antioxidants," *Food Technol. Biotechnol.*, vol. 57, no. 1, 2019. Available: https:// doi.org/10.17113/ftb.57.01.19.5784

[3] A. Sadeghi, A. Rajabiyan, N. Nabizade, N. Meygolinezhad, and A. Z. Ahmady, "Seaweed-derived phenolic compounds as diverse bioactive molecules: A review on identification, application, extraction and purification strategies," *Int. J. Biol. Macromol.*, p. 131147, Mar. 2024. Available: https:// doi.org/10.1016/J.IJBIOMAC.2024.131147

[4] P. A. Uwineza and A. Waśkiewicz, "Recent advances in supercritical fluid extraction of natural bioactive compounds from natural plant materials," Sep. 2020, *MDPI AG*. Available: https:// doi.org/10.3390/molecules25173847

[5] A. Abu-Nada, A. Abdala, and G. McKay, "Removal of phenols and dyes from aqueous solutions using graphene and graphene composite adsorption: A review," Oct. 2021, *Elsevier Ltd*. Available: https:// doi.org/10.1016/j.jece.2021.105858

[6] H. N. Catherine, M. H. Ou, B. Manu, and Y. hsin Shih, "Adsorption mechanism of emerging and conventional phenolic compounds on graphene oxide nanoflakes in water," *Science of the Total Environment*, vol. 635, pp. 629–638, Sep. 2018. Available: https:// doi.org/10.1016/j.scitotenv.2018.03.389.

[7] A. A. Jabbar *et al.*, "Extremely efficient aerogels of graphene oxide/graphene oxide nanoribbons/sodium alginate for uranium removal from wastewater solution," *Scientific Reports 2024 14:1*, vol. 14, no. 1, pp. 1–9, Jan. 2024. Available: https://doi.org/10.1038/s41598-024-52043-1

https://doi.org/10.24191/esteem.v22iMarch.4737

[8] Y. GadelHak, M. El-Azazy, M. F. Shibl, and R. K. Mahmoud, "Cost estimation of synthesis and utilization of nano-adsorbents on the laboratory and industrial scales: A detailed review, *Elsevier B.V.* vol. 875, p. 162629, Jun 2023. Available: https:// doi.org/10.1016/j.scitotenv.2023.162629

[9] C. Jiang *et al.*, "Study on Application of Activated Carbon in Water Treatment," in *IOP Conference Series: Earth and Environmental Science*, vol. 237, p. 022049, Mar. 2019. Available: https:// doi.org/10.1088/1755-1315/237/2/022049

[10] A. Avornyo and C. V. Chrysikopoulos, "Applications of graphene oxide (GO) in oily wastewater treatment: Recent developments, challenges, and opportunities," *Journal of Environmental Management*, vol. 353, p. 120178, Feb. 2024, *Academic Press*. Available: https:// doi.org/10.1016/j.jenvman.2024.120178

[11] M. S. Islam, H. Roy, T. Ahmed, S. H. Firoz, and S. X. Chang, "Surface-modified graphene oxide-based composites for advanced sequestration of basic blue 41 from aqueous solution," *Chemosphere*, vol. 340, Nov. 2023. Available: https:// doi.org/10.1016/j.chemosphere.2023.139827

[12] K. Yokwana, B. Ntsendwana, E. N. Nxumalo, and S. D. Mhlanga, "Recent advances in nitrogen-doped graphene oxide nanomaterials: Synthesis and applications in energy storage, sensor electrochemical applications and water treatment," *Journal of Materials Research*, vol. 38, pp. 3239–3263, Jun. 2023. Available: https:// doi.org/10.1557/s43578-023-01070-1

[13] M. Jain *et al.*, "Modelling and statistical interpretation of phenol adsorption behaviour of 3-Dimensional hybrid aerogel of waste-derived carbon nanotubes and graphene oxide," *Chemical Engineering Journal*, vol. 490, Jun. 2024. Available: https:// doi.org/10.1016/j.cej.2024.151351

[14] M. A. M. Ariff, A. M. Yusri, N. A. A. Razak, and J. Jaapar, "Effect of CO2 flow rate, co-solvent and pressure behavior to yield by supercritical CO2 extraction of Mariposa Christia Vespertilionis leaves," in *AIP Conference Proceedings*, vol. 2045, no. 1, p. 020072 Dec. 2018. Available: https:// doi.org/10.1063/1.5080885

[15] A. Javed, S. R. Abbas, M. U. Hashmi, N. U. A. Babar, and I. Hussain, "Graphene oxide based electrochemical genosensor for label free detection of mycobacterium tuberculosis from raw clinical samples," *Int. J. Nanomedicine*, vol. 16, pp. 7339–7352, 2021. Available: https:// doi.org/ 10.2147/IJN.S326480

[16] M. Subramaniam, A. R. Mohamed, and S. Y. Lai, "One-pot synthesis of regenerative calcium counterions from waste chicken eggshells for SO2-to-sulfur reduction," *Materials Today Sustainability*, vol. 26, Jun. 2024. Available: https:// doi.org/10.1016/j.mtsust.2024.100749

[17] D. A. Rahim *et al.*, "Microwave-assisted synthesis of Zn-Fe adsorbent supported on alumina: Effect of Zn to Fe ratio on syngas desulfurization performance," *Chemical Engineering and Processing - Process Intensification*, vol. 168, Nov. 2021. Available: https:// doi.org/10.1016/j.cep.2021.108565

[18] M. P. Kodjapashis *et al.*, "Isolation and identification of olive tree leaf phenols through a resin adsorption/desorption process," *Sustain. Chem. Pharm.*, vol. 38, Apr. 2024. Available: https:// doi.org/10.1016/j.scp.2024.101484

[19] S. Burapan, M. Kim, Y. Paisooksantivatana, B. E. Eser, and J. Han, "Thai Curcuma Species: Antioxidant and Bioactive Compounds," *Foods,* vol. 9, no. 9, p. 1219, Sep. 2020. Available: https:// doi.org/10.3390/FOODS9091219

[20] M. Movafaghi Ardestani, B. Forouzesh Rad, S. Mahpishanian, M. Baghdadi, and B. Aminzadeh Goharrizi, "A Surface Modification of Chemically Expanded Graphite with Pyrrole and Dithiocarbamate and Its Application for Adsorption of Hg2+ from Synthetic Wastewater: Isotherm, Kinetics, and Thermodynamic Studies," *Water Air Soil Pollut.*, vol. 234, Aug. 2023. 10.1007/s11270-023-06539-7

https://doi.org/10.24191/esteem.v22iMarch.4737

[21] Y. Tian, N. Zhang, Y. Liu, W. Chen, R. Lv, and H. Ma, "Adsorption performance of expanded graphite and its binary composite microbeads toward oil and dyes," *Desalination Water Treat.*, vol. 178, pp. 283–295, Feb. 2020. Available: https://doi.org/10.5004/dwt.2020.24937

[22] T. Phatthanakittiphong and G. T. Seo, "Characteristic evaluation of graphene oxide for bisphenol a adsorption in aqueous solution," *Nanomaterials*, vol. 6, Jul. 2016. Available: https:// doi.org/10.3390/nano6070128

[23] H. V. T. Luong, T. P. Le, T. L. T. Le, H. G. Dang, and T. B. Q. Tran, "A graphene oxide based composite granule for methylene blue separation from aqueous solution: Adsorption, kinetics and thermodynamic studies," *Heliyon*, vol. 10, Apr. 2024. Available: https:// doi.org/10.1016/j.heliyon.2024.e28648

[24] T. Song *et al.*, "Adsorption Behaviors of Polycyclic Aromatic Hydrocarbons and Oxygen Derivatives in Wastewater on N-Doped Reduced Graphene Oxide," *Sep. Purif. Technol.*, vol. 254, Jan. 2021. Available: https:// doi.org/10.1016/j.seppur.2020.117565

[25] M. Utami *et al.*, "Simultaneous photocatalytic removal of organic dye and heavy metal from textile wastewater over N-doped TiO2 on reduced graphene oxide," *Chemosphere*, vol. 332, Aug. 2023. Available: https:// doi.org/10.1016/j.chemosphere.2023.138882

[26] W. T. Tee *et al.*, "A high-performance 3D phosphorus-doped graphene oxide adsorbent for imipramine wastewater treatment," *Sep. Purif. Technol.*, vol. 330, Feb. 2024. Available: https:// doi.org/10.1016/j.seppur.2023.125266

[27] B. Anegbe, I. H. Ifijen, M. Maliki, I. E. Uwidia, and A. I. Aigbodion, "Graphene oxide synthesis and applications in emerging contaminant removal: a comprehensive review," *Environ Sci Eur*, vol. 36, no. 15, Dec. 2024. Available: https:// doi.org/10.1186/s12302-023-00814-4

[28] N. Wu, X. Zhang, X. Zhang, K. Yang, and Y. Li, "Simultaneous degradation of trace antibiotics in water by adsorption and catalytic oxidation induced by N-doped reduced graphene oxide (N-rGO): synergistic mechanism," *Mater. Res. Express*, vol. 9, Jun. 2022. Available: https:// doi.org/10.1088/2053-1591/ac7284

[29] N. Wu, X. Zhang, X. Zhang, K. Yang, and Y. Li, "Simultaneous degradation of trace antibiotics in water by adsorption and catalytic oxidation induced by N-doped reduced graphene oxide (N-rGO): synergistic mechanism," *Mater. Res. Express*, vol. 9, no. 6, Jun. 2022. Available: https:// doi.org/10.1088/2053-1591/AC7284

[30] S. Khaliha *et al.*, "Graphene oxide nanosheets for drinking water purification by tandem adsorption and microfiltration," *Sep. Purif. Technol.*, vol. 300, Nov. 2022. Available: https:// doi.org/10.1016/j.seppur.2022.121826

[31] K. Jayakumar *et al.*, "One-step electrochemical preparation of platinum nanoparticle decorated self-healing reduced graphene oxide three-dimensional nanoarray for portable detection of bisphenol A," *J. Environ. Chem. Eng.*, vol. 12, no. 5, Oct. 2024. Available: https:// doi.org/10.1016/j.jece.2024.113518

[32] M. A. Ahmad Farid, J. Lease, and Y. Andou, "Behaviour and mechanics of phenolic sorption by novel bio-based graphene derivatives as adsorbents," *Chemosphere*, vol. 366, Oct. 2024. Available: https:// doi.org/10.1016/j.chemosphere.2024.143490

[33] X. Gong *et al.*, "One-Step Synthesis of 3D Nitrogen-doped Graphene Quantum Dots and Reduced Graphene Oxide Composites by a Hydrothermal Method for Supercapacitors Anodes," Mar. 2023. Available: https:// doi.org/10.21203/rs.3.rs-2667742/v1

[34] F. T. Johra and W. G. Jung, "Hydrothermally reduced graphene oxide as a supercapacitor," *Appl. Surf. Sci.*, vol. 357, pp. 1911–1914, Dec. 2015. Available: https:// doi.org/10.1016/j.apsusc.2015.09.128

https://doi.org/10.24191/esteem.v22iMarch.4737

[35] W. Tang *et al.*, "Facile synthesis of 3D reduced graphene oxide and its polyaniline composite for super capacitor application," *Synth. Met.*, vol. 202, pp. 140–146, 2015. Available: https://doi.org/10.1016/j.synthmet.2015.01.031

[36] K. Tian, Z. Su, H. Wang, X. Tian, W. Huang, and C. Xiao, "N-doped reduced graphene oxide/waterborne polyurethane composites prepared by in situ chemical reduction of graphene oxide," *Compos. Part A Appl. Sci. Manuf.*, vol. 94, pp. 41–49, Mar. 2017. Available: https://doi.org/10.1016/j.compositesa.2016.11.020

https://doi.org/10.24191/esteem.v22iMarch.4737